Engineering Failure Analysis 147 (2023) 107154

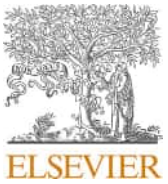

Contents lists available at ScienceDirect

Engineering Failure Analysis

journal homepage: www.elsevier.com/locate/engfailanal

Combined use of deformation and structural analysis for the structural damage assessment of heritage buildings: A case study in the Liguria region (Italy)

Giulio Lucio Sergio Sacco, Chiara Ferrero *, Carlo Battini, Chiara Calderini

Department of Civil, Chemical and Environmental Engineering, University of Genoa, Via Montallegro 1, 16145 Genoa, Italy

ARTICLE INFO

Keywords:
Historic masonry churches
Slow-moving landslides
Foundation settlements
Deformation analysis
Finite element modelling
Damage assessment

ABSTRACT

Cultural heritage buildings as they appear today are the result of continuous transformations occurred over the centuries. For this reason, their structural assessment should integrate structural analysis with a deep knowledge of the building history, actual geometry, damage, past alterations, and actions undergone over time. This paper presents the structural damage assessment of San Carlo Borromeo church, a historic masonry building located in the Liguria region (Italy) in a slow-moving landslide-affected area. To assess the effect of the landslide and identify the causes of the damage and deformations observed in the building, structural analysis was combined with historical research, on-site inspections, laser scanner survey and deformation analysis. A finite element model of the entire church in its geometric undeformed configuration was prepared by removing all the deformations identified through the deformation analysis from the actual deformed geometry obtained from the laser scanner survey. Nonlinear static analyses were then performed by applying at the base of the model a set of displacement fields obtained from the deformation analysis and representing the displacements experienced by the building due to the landslide and further phenomena that were found to have occurred. The damage and deformations predicted numerically were compared with those detected in the church. The good agreement proved that the deformation analysis is an effective tool to support structural analysis and assess the actual deformations and displacements experienced by historic masonry constructions.

1. Introduction

The preservation of historic masonry buildings requires structural analysis, which is essential to assess their structural behaviour, identify the causes of existing damage and deformations, design strengthening interventions and plan risk mitigation strategies. Despite the recent advances in computational methods, the structural analysis of heritage constructions is still a demanding task due to the difficulties in modelling complex materials and geometries and the need to adequately consider the history of the building and the actions which it has undergone during its lifespan [1]. Over time, historic masonry buildings may have been subjected to a range of actions, either natural (e.g., earthquakes, landslides, hurricanes) or anthropogenic (e.g., architectural alterations, intentional

* Corresponding author.
E-mail addresses: giuliolucio sergio.sacco@edu.unige.it (G.L.S. Sacco), chiara.ferrero@edu.unige.it (C. Ferrero), carlo.battini@unige.it (C. Battini), chiara.calderini@unige.it (C. Calderini).

https://doi.org/10.1016/j.engfailanal.2023.107154
Received 17 January 2023; Received in revised form 1 February 2023; Accepted 24 February 2023
Available online 26 February 2023

destruction) [2]. The combination of these actions with gravity loading, construction process, long-term creep, soil settlements, and material degradation produces a gradual transformation of the building and may result in damage and deformations [1]. Since these deformations may be several orders of magnitude larger than those estimated through standard structural analysis [3], they should be considered to accurately assess the current equilibrium condition of heritage structures and evaluate their response to static or seismic loading.

In the literature, several authors performed the structural assessment and analysis of historic masonry buildings taking into account their history, construction process and/or geometric deformation. To provide some examples, in [4], the influence of construction process and long-term deformations on the static and seismic response of a historic masonry cathedral was assessed through finite element (FE) simulations. In [5], the effect of geometric imperfections and deformations on the seismic response of a historic masonry mosque was evaluated by comparing the numerical results from two FE models, one with a simplified geometry obtained from traditional geometric measurements and the other with a more accurate geometry derived from terrestrial laser scanning. In [6] and [7], the structural damage of a historic masonry church was assessed by preparing a numerical model that included the building actual deformed geometry (obtained from terrestrial laser scanning) and performing numerical analyses under different scenarios that may have affected structural integrity (e.g., gravitational loading, differential settlements, seismic actions, and past structural alterations).

Very recently, slow-moving landslides have been observed to produce large deformations in historic masonry churches [8 9]. Slow-moving landslides are characterized by a slow kinematics and have a typical velocity ranging from a few mm/year to 1.6 m/year [10 11]. Although they result in soil and building movements that are very small in their instantaneous value, they may move downslope for years to decades (and even centuries), causing displacements to accumulate over time. The accumulated displacements may produce severe damage and large deformations to masonry structures (see e.g., [12 13 14 15]), especially heritage buildings and, among them, historic masonry churches [8 9].

So far, a few research works have dealt with the damage assessment and structural analysis of historic masonry churches exposed to slow-moving landslides and none of them has thoroughly investigated and quantified the deformations resulting from landslide movements. In [16], an integrated approach combining Synthetic Aperture Radar (SAR) tomography with laser scanner acquisition and structural analysis was proposed to investigate the damage mechanisms of a historic masonry cathedral exposed to slow-moving landslide phenomena. In [8] and [9], the structural response of a large sample of 33 churches located in the Liguria region (Italy) in areas affected by slow-moving landslides was investigated. Recurrent damage mechanisms were identified by performing a qualitative damage assessment, in which the congruence between damage and landslide direction was evaluated based on engineering judgement and cracks were used as indicators of ground movements. In [17], the damage mechanisms identified in [8] and [9] were presented in further detail through the critical analysis of some case studies. In [18] and [19], the effect of slow-moving landslides on historic masonry churches was assessed by performing geotechnical analyses on some case studies selected among the churches investigated in [8] and [9]. The landslide-induced soil and building displacements were deeply investigated, while the structural response of the churches, modelled as elastic blocks, was not analysed.

This paper presents the structural damage assessment of a historic masonry church, San Carlo Borromeo church, located in the Liguria region (Italy) in an area affected by a slow-moving landslide. The church, which belongs to the set of buildings investigated in [8] and [9], exhibits extensive cracks and large deformations that are not fully congruent with the direction of the acting landslide. To assess the effect of the slow-moving landslide and identify further phenomena that could be responsible for damage and deformations, structural analysis was combined with historical research, on-site inspections, laser scanner survey and deformation analysis.

Historical research was carried out to identify the construction phases and the architectural/structural alterations undergone by the church over time. On-site inspections were performed with the twofold aim of surveying in detail the crack patterns and gathering information about geometric features, structural details, and materials. The laser scanner survey was performed to obtain the actual geometry of the structure with a high level of accuracy (about 1 mm). Based on the point cloud derived from the laser scanner survey, a deformation analysis was carried out with the aim of assessing the deformations experienced by the structure over time. Such deformations were evaluated by comparing the real (deformed) geometry of the church with a reference (undeformed) geometry, which was specifically reconstructed. As main novelty of this work, the deformation analysis led to the identification of a set of displacement fields representative of the displacements induced by the slow-moving landslide and further phenomena that were found to have occurred (i.e., differential foundation settlements). These displacement fields were used to perform structural analysis.

A finite element (FE) model of the entire church in its geometric undeformed configuration was prepared. A macro-modelling approach was adopted to represent masonry. Nonlinear static analyses were performed by imposing the displacement fields identified through the deformation analysis according to a sequence that takes into consideration the history and construction phases of San Carlo Borromeo church. The response of the building to the slow-moving landslide and foundation settlements was analysed in terms of crack patterns and deformations, which were represented through the distribution of maximum principal plastic strain and total displacement, respectively. The numerical results were then compared with the real crack patterns and deformations observed in the church to prove the capacity of the numerical model to reproduce the current damage state and to verify the accuracy of the displacements fields identified through the deformation analysis.

This paper is organized as follows. Section 2 provides a description of San Carlo Borromeo church and the geotechnical and landslide settings of the area where the building is located. Section 3 focuses on the damage and deformations exhibited by the structure. First, the crack patterns observed during on-site inspections are described. Then, the procedure and results of the deformation analysis are presented. Finally, the detected crack patterns and deformations are critically analysed and the displacement fields to be used in the structural analysis are identified. Section 4 presents the structural analysis. First, the preparation of the numerical model is described. Then, the results of the numerical analyses are presented. Lastly, the real and predicted crack patterns and deformations are compared.

2. San Carlo Borromeo church in Cassingheno

2.1. Description of the building

San Carlo Borromeo church (Fig. 1) is located in Cassingheno, a small village in the municipality of Fascia (Genoa metropolitan area, Liguria region). The church has a single nave, a presbytery, a semi-circular apse, two lateral chapels and a belltower (see Fig. 2). It is about 21.5 m long and has a width varying from 6.2 to 7.7 m (Fig. 2a). As shown in Fig. 2a, two adjacent buildings (a clergy house and a sacristy) are present on the left (north-western) side of the church. The nave and the presbytery, which are separated by a triumphal arch, are covered with barrel vaults, while the apse has a hemispherical dome. Five metallic tie-rods are present, four located at the springings of the transverse arches and one running along the inner side of the façade wall (see Fig. 2a). The entire building (both walls and vaults) is made of stone masonry and is covered by a wooden roof, which was recently rebuilt.

San Carlo Borromeo church as it appears today is the result of significant transformations undergone over time (Fig. 3). Different construction phases were identified through historical research and archaeological/stratigraphical analysis. Although the first document attesting the existence of the building as an oratory dates back to 1595 [20], it is likely that the original core of the church was built in the late Middle Ages [21]. The original building is expected to be similar in shape to the current one but smaller and with a shorter belltower (compare Fig. 3a and b). The current apse, presbytery and lower part of the belltower (up to the belfry) are the only remaining parts of the original building. The current nave, whose walls are not aligned with those of the apse, was constructed at a later time (before 1595) and is larger than the original one (compare Fig. 3a and b). It is likely that the current belfry was added at the same time of the enlargement of the nave or just after, leading to the configuration shown in Fig. 3b. Subsequently, before 1879, a sacristy and a chapel were added on the left (north-western) and right (south-eastern) sides of the church, respectively (Fig. 3c). Between the end of the nineteenth century and the first half of the twentieth century, San Carlo Borromeo church underwent further

Fig. 1. San Carlo Borromeo church: a) south-eastern façade, b) front façade, c) interior.

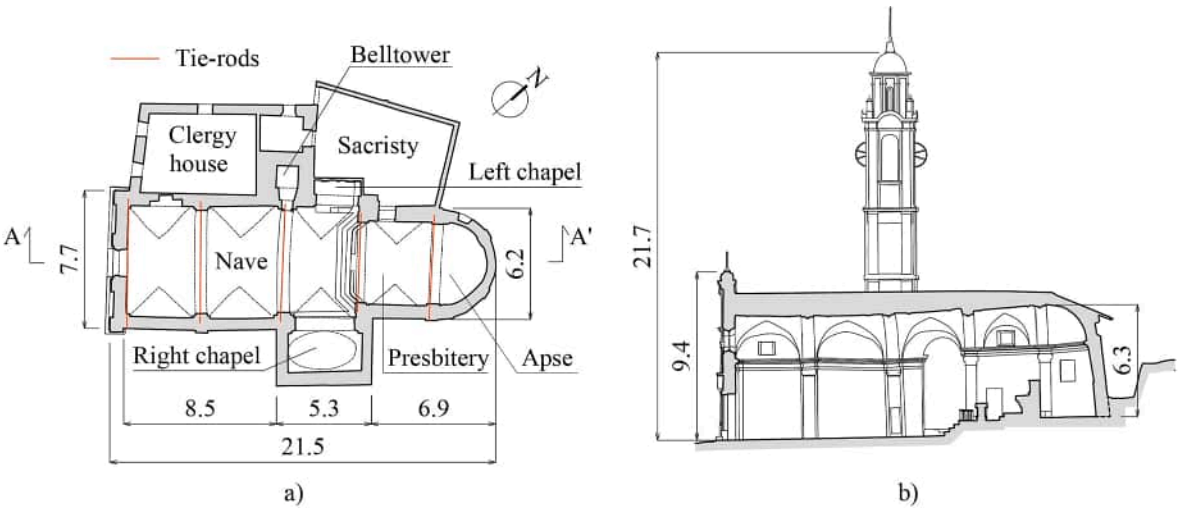

Fig. 2. Geometry of San Carlo Borromeo church: a) plan, b) section AA'.

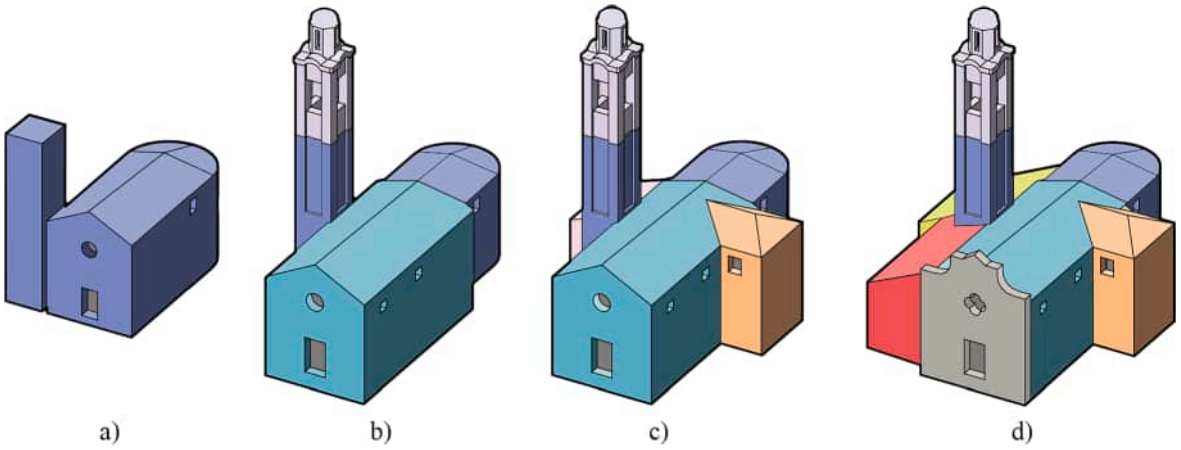

Fig. 3. Transformations of San Carlo Borromeo church over time: a) original building - late Middle Ages, b) construction of the current nave and belfry – before 1595, c) addition of the sacristy and the right chapel – before 1879, d) current configuration.

transformations, which included the construction of the clergy house (coloured in red in Fig. 3d), the reconstruction of the original sacristy and the renovation of the façade. These transformations brought the building to its present form, which is shown in Fig. 3d. Further restoration interventions such as the refurbishment of the floor and the straightening of the belltower were carried out in the twentieth century [22]. For the purpose of this work, it should be noted that no information about past damage due to earthquakes emerged from the historic research carried out by the authors. This is in agreement with the medium–low seismicity of the area where Cassingheno village is located (see the Italian seismic zoning updated to 2022, [23]).

2.2. Geotechnical and landslide settings

San Carlo Borromeo church and the village of Cassingheno are located on a slope with medium–low inclination (about 20° to the horizontal), which is likely to be the accumulation zone of a relict deep slide. In the area of interest, the soil consists of a thick layer (10–15 m) of very heterogeneous blanket (sand with clasts and clayey silts), which is separated from the bedrock (shales) by a transition zone (1–3 m thick) of weathered rock. The ground water table, which oscillates according to the seasonality, is located within the blanket [18].

As shown in Fig. 4a-b, the entire village of Cassingheno lies on an active slow-moving landslide, which has an area of about 0.17 km^2 [24] and is classified as complex [25]. According to the *Atlas of the Unstable Inhabited Centres of Liguria (Atlante dei Centri Instabili della Liguria*, hereafter called *Atlante*, [25]), the landslide caused damage to several buildings of Cassingheno village, including San Carlo Borromeo church. Fig. 4 shows the direction of this landslide (indicated with an arrow), which was estimated on the basis of the

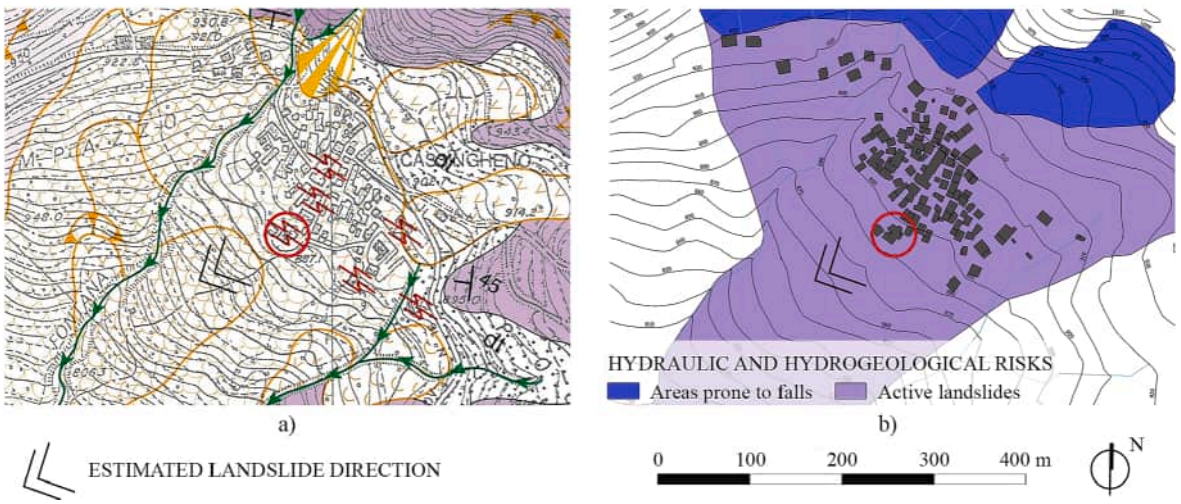

Fig. 4. Landslide maps for the landslide affecting Cassingheno village and San Carlo Borromeo church (indicated with a red circle): a) *Atlante dei Centri Instabili della Liguria* [25], b) *Atlante dei Rischi Idraulici e Idrogeologici* (adapted from [26]). (For interpretation of the references to colour in this figure legend, the reader is referred to the web version of this article.)

orientation of the symbols used in the *Atlante* to represent landslide phenomena, as suggested in [8]. For the purpose of this work, it is interesting to observe that the landslide direction is almost parallel to the longitudinal axis of San Carlo Borromeo church.

Between 2014 and 2017, the slow-moving landslide affecting Cassingheno village was monitored by means of a system of inclinometers, which were installed within the framework of the REMOVER monitoring project of the Liguria Region. All the inclinometers showed small movements of the blanket at variable depths along the slope and indicated a possible failure surface at a depth of about 9–12 m from the ground surface [19].

3. Damage and deformations

3.1. Crack pattern survey

The crack patterns surveyed in San Carlo Borromeo church are presented in plan and elevation in Fig. 5a-b-c. The cracks were classified according to three levels of width: (i) thin for a width up to 1 mm (the latter included), (ii) medium for a width between 1 and 5 mm, and (iii) large for a width equal or larger than 5 mm. The most representative damages are illustrated in Fig. 5d-e-f-g. In 2019, the church underwent a restoration that partially hided the damage on the exteriors. For this reason, the crack patterns observed by the authors in 2020 were integrated with those reported in [8], which date back to 2018.

Severe and extensive damage was observed in the walls. In the nave, the most significant damage was detected in the second bay behind the façade. In this bay, the left (north-western) longitudinal wall is affected by a series of medium to large diagonal cracks progressing upwards towards the apse (see Fig. 5a-d). One of these cracks develops from the level of the ground. Similarly, the right (south-eastern) longitudinal wall exhibits a series of medium to large diagonal cracks propagating from the level of the floor and developing upwards towards the apse (Fig. 5b-e). In addition to these cracking patterns, vertical or slightly inclined cracks developing upwards from the level of the ground are observed in the right longitudinal walls of presbytery, apse, and first bay of the nave behind the façade (see Fig. 5b). Lastly, two large cracks are present in the left longitudinal walls, one located in the first bay behind the façade and the other in the presbytery (Fig. 5a). Both cracks are diagonal and progress upwards towards the façade. The crack in the presbytery was repointed before 2018 and no sign of partial reopening was observed in either 2018 or 2020.

Severe damage was observed also in the floor. In the second bay behind the façade, a large crack (about 12 mm wide) cuts the floor of the entire nave, propagating transversally between the longitudinal walls (see blue line in Fig. 5c-f). This crack is in continuity with the cracks affecting the longitudinal walls. Thin to medium cracks, oriented perpendicular to the direction of the landslide acting in the area, were also observed in the floor of the first bay and the northernmost part of the right chapel (see blue lines in Fig. 5c).

Differently from walls and floor, arches and vaults do not exhibit severe cracking (see Fig. 5c). A thin to medium longitudinal crack, oriented in same direction as the landslide, cuts the barrel vaults of nave and presbytery approximately at mid-span (Fig. 5c-g). This crack changes direction while progressing towards the left longitudinal wall of the nave on one side and the wall of the presbytery on the other side. Thin cracks with a slight concentric pattern are also detected around the belltower (Fig. 5c). Lastly, very thin diagonal cracks are widespread in the nave, presbytery, and right chapel.

3.2. Deformation analysis

A deformation analysis was performed with the aim of assessing and quantifying the deformations experienced by San Carlo Borromeo church during its lifespan. Such deformations were evaluated in terms of distance or rotation between the current and reference geometric configurations of a number of architectural elements composing the church (walls, arches, mouldings, floors, etc.). A laser scanner survey provided the current geometric configuration of the entire building in the form of a point-cloud.

The laser scanner survey campaign was conducted in May 2019 by using the Z + F 5006 h laser scanner and the Topcon GPT-2006 total station. This laser scanner guaranteed the acquisition of about 25 million points for each station with a panoramic coverage of 360° on the horizontal and 310° on the vertical, allowing the actual geometry of the church to be recorded with an accuracy of about 1 mm for each point surveyed. Eighty-one scans were made and then aligned within Autodesk's Recap Pro software by using cloud to cloud algorithms as well as the points recorded through the topographic station. The topographical station guaranteed the identification of a perfect horizontality and, therefore, a perfect registration of the out-of-plumbness of the analysed structure. The result was a database of approximately 800 million points of San Carlo Borromeo church with a global registration error of 4.54 mm.

The deformation analysis of San Carlo Borromeo church was carried out by analysing eight sections: (i) two longitudinal sections (AA' and BB'), made along the same longitudinal axis (Fig. 6), (ii) four transverse sections (CC', DD', EE', FF'), located in correspondence of the transverse arches and orthogonal to the longitudinal sections (Fig. 7), and (iii) two sections (one longitudinal, GG', and one transverse, HH') passing through the right chapel (Fig. 9). The floor of the nave was also investigated within the scope of the deformation analysis.

The deformation analysis of the longitudinal sections is shown in Fig. 6. Walls, pilasters, vaults, mouldings, and floors were chosen as the architectural elements to be analysed. For each element, the deformation was estimated by choosing a reference pole of rotation (orange dot in Fig. 6) and a reference line representing the undeformed reference configuration (blue dashed line in Fig. 6) and measuring the rotation between the reference geometry and the surveyed one. The reference line was assumed to be vertical for walls and pilasters and horizontal for floor and mouldings. In the case of the vault of the nave, which exhibits a significant deformation (solid red line in Fig. 6, amplified by ten times), the rotation was measured between the horizontal reference line and a line connecting the two extremities of the vault (orange dashed line in Fig. 6). As shown in Fig. 6, all the architectural elements analysed exhibit a rotation towards valley, in the direction of the slow-moving landslide. This outcome clearly indicates that the entire church experienced a

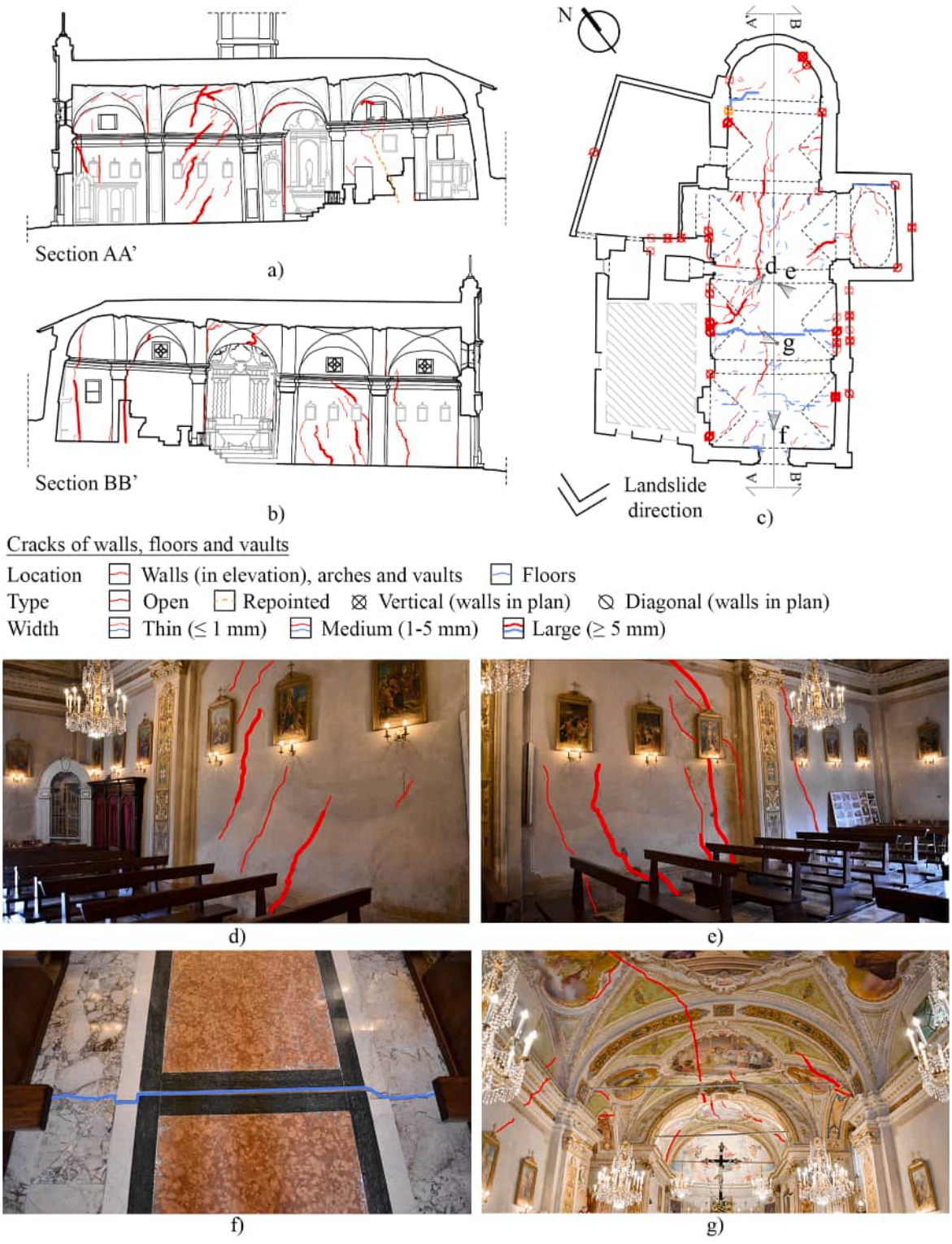

Fig. 5. Damage survey of San Carlo Borromeo church in Cassingheno: a) crack pattern in plan (the direction of the slow-moving landslide acting in the area is indicated with an arrow), b) crack pattern in elevation (section AA', left longitudinal wall), c) crack pattern in elevation (section BB', right longitudinal wall), d-e) diagonal cracks in the left (d) and right (e) longitudinal walls of the nave (second bay behind the façade), e) large crack in the floor of the nave, f) cracks in arches and vaults.

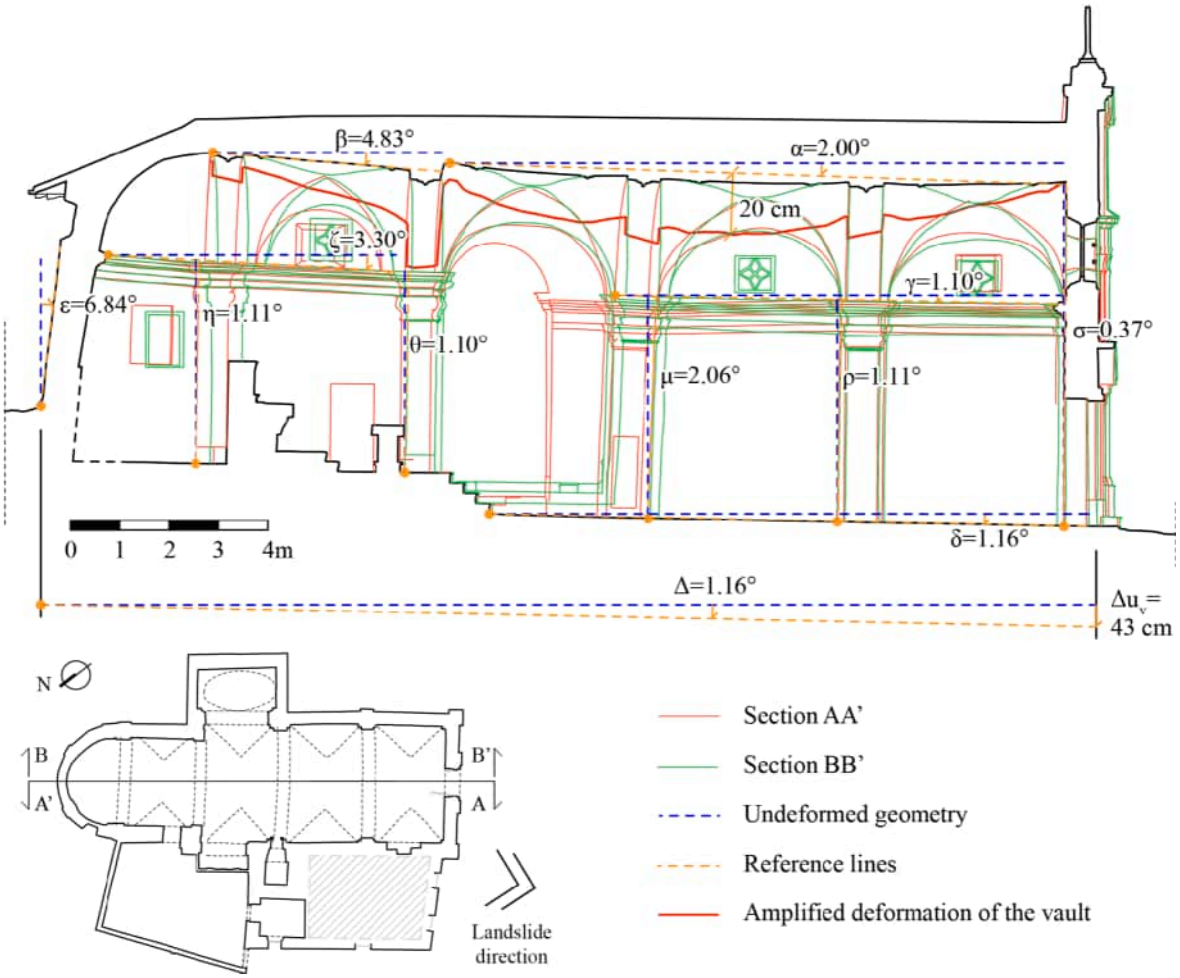

Fig. 6. Deformation analysis of the longitudinal sections of San Carlo Borromeo church: superimposition of sections AA' and BB'. (Deformed geometry of the vault amplified by 10 times).

global rotation in this direction. The most significant rotations were observed in the apse and presbytery. The vault of the presbytery, the apse wall, and the mouldings were found to be rotated with respect to the vertical by about 4.83° (see angle β in Fig. 6), 6.84° (angle ε), and 3.30° (angle ζ), respectively. In the nave, the floor and the mouldings show a smaller rotation of 1.16° (angle δ) and 1.10° (angle γ), respectively, while the barrel vault exhibits a rotation of 2.00° (angle α) in addition to a deflection of about 20 cm in the centre of the second bay (see Fig. 6). All the pilasters present a rotation of about 1.1° except for the second one from the façade, which shows a larger rotation (2.06°, angle μ). No significant rotations were detected in the façade. The larger rotations measured in the presbytery and apse compared to the nave can be explained considering that the presbytery and the apse were built before the nave and, thus, they may have experienced deformations for a longer period of time (see Section 2.1). Due to the uncertainties about the historical information, the rotation of the floor of the nave was conservatively chosen to represent the overall rotation experienced by the church. By applying a rotation of 1.16° to the whole church and placing the rotation pole at the exterior of the apse (see angle Δ in Fig. 6), the vertical displacement between the apse and the façade (Δu_v) can be estimated at about 43 cm.

The deformation analysis of the transverse sections of San Carlo Borromeo church is illustrated in Fig. 7. Walls and arches were chosen as the architectural elements to be investigated. The deformation of the longitudinal walls was estimated in terms of rotation between a vertical reference line representing the undeformed configuration (blue dashed line) and an inclined line (orange dashed line) representing the deformed geometry (red solid line, amplified by ten times). This inclined line was obtained by connecting the rotation pole (orange dot) at the base of the wall with the top point of the wall in the deformed configuration.

The deformation of the transverse arches was evaluated in terms of vertical and horizontal displacements of both the springings and the crown and was obtained by comparing the real deformed geometry derived from the laser scanner survey (red solid line, amplified by ten times in Fig. 7) with a reference undeformed geometry, which was assumed to be elliptical (blue dashed line in Fig. 7). The reference undeformed geometry was found by imposing that the intrados length of the undeformed arch was equal to the intrados length of the real deformed arch and the span of the undeformed arch was equal to the distance between the longitudinal walls in their (vertical) undeformed configuration. To perform the deformation analysis of the transverse arches, a Grasshopper script was developed

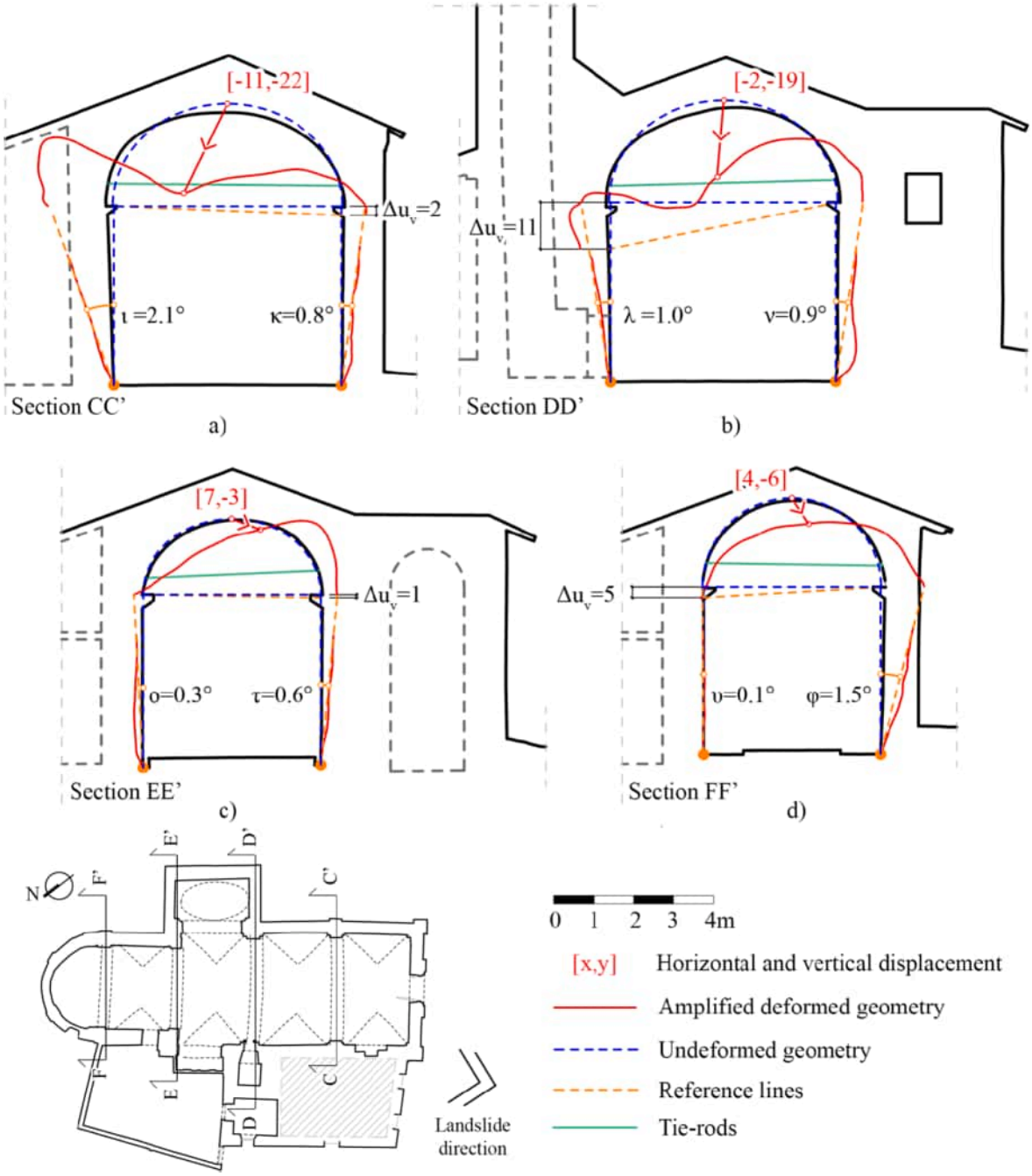

Fig. 7. Deformation analysis of the transverse sections of San Carlo Borromeo church: a) section CC', b) section DD', c) section EE', d) section FF'. (Displacements at the arch springings Δu_v shown in cm; deformed geometry amplified by 10 times).

in Rhinoceros 7 [27] (see Fig. 8). The arch surveyed geometry and undeformed span were used as input of the script (see green blocks in Fig. 8) with the twofold aim of reconstructing the arch undeformed geometry (see purple block in Fig. 8) and estimating the arch deformation in terms of displacements of both the springings and crown (see blue block in Fig. 8). An optimisation add-on component for Grasshopper named Goat was used for the arch reconstruction.

The deformation analysis of the transverse sections allowed different deformation phenomena to be identified. First, in sections CC' (Fig. 7a) and DD' (Fig. 7b), both the longitudinal walls were found to present a significant out-of-plumb towards the exterior of the building. Differently, in section EE' (Fig. 7c) and FF' (Fig. 7d), only the right longitudinal wall was observed to lean towards the exterior. Second, the arches of the nave (section CC' and DD' in Fig. 7a-b, respectively) appear to be the most deformed ones, as they exhibit a vertical displacement at the crown that is significantly larger than that of the arches of the apse and presbytery (sections EE'

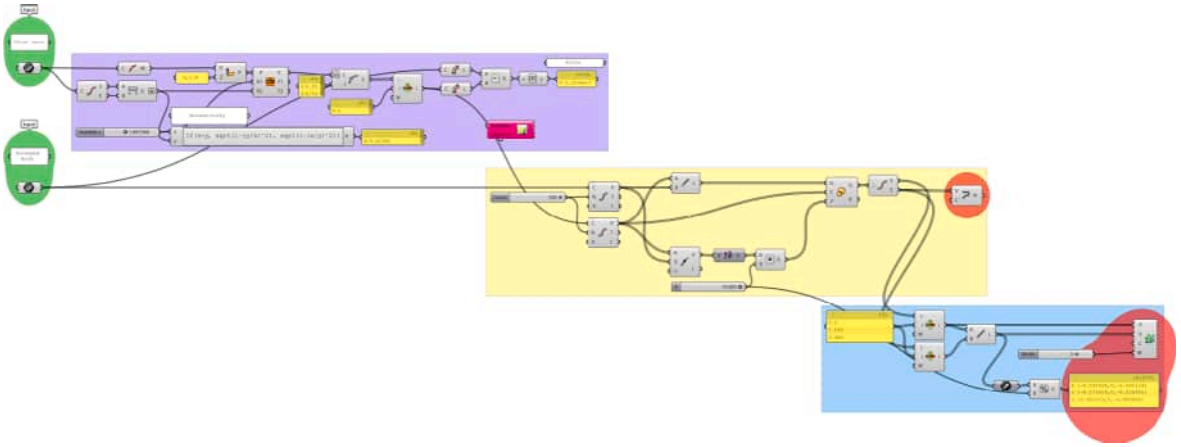

Fig. 8. Grasshopper script for the deformation analysis of the transverse arches. Green: inputs; purple: arch reconstruction; yellow: deformation amplification; blue: evaluation of the displacements of the springings and crown; red: outputs. (For interpretation of the references to colour in this figure legend, the reader is referred to the web version of this article.)

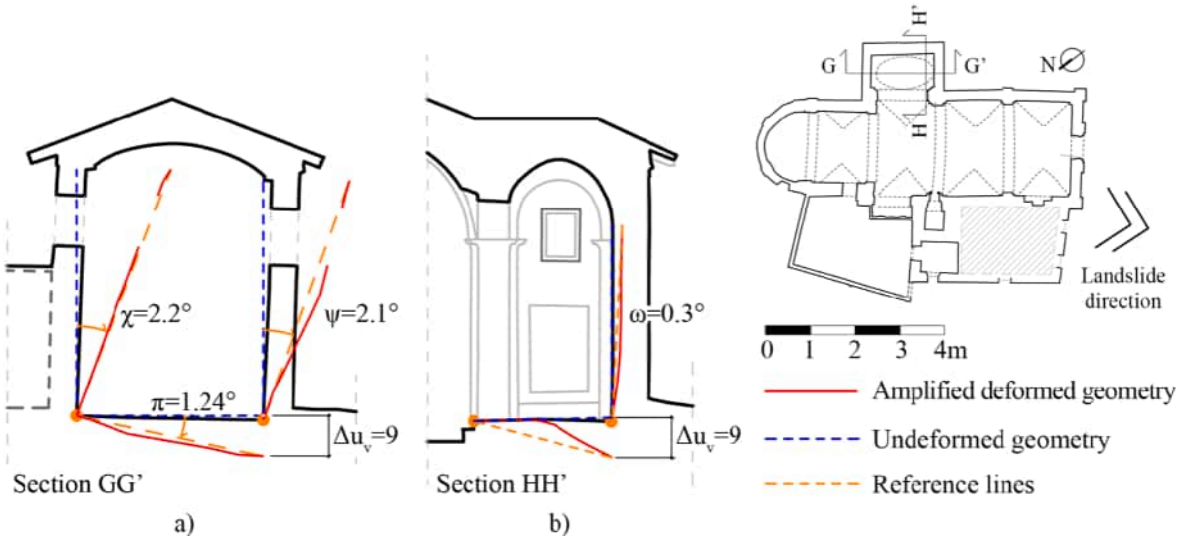

Fig. 9. Deformation analysis of the right chapel of San Carlo Borromeo church: a) section GG', b) section HH'. (Vertical displacements of the floor Δu_v shown in cm; deformed geometry amplified by 10 times).

and FF' in Fig. 7c-d, respectively). This vertical displacement is consistent with the deflection of the barrel vault measured in the longitudinal sections (about 20 cm). Third, the left springing of the arches of sections DD' (Fig. 7b) and FF' (Fig. 7d) settled vertically with respect to the right springing. The largest settlement was observed in correspondence of the belltower (11 cm, see section DD' in Fig. 7b), while a smaller settlement of about 5 cm was found between apse and presbytery (5 cm, see section FF' in Fig. 7d). These vertical settlements suggest the occurrence of a differential foundation settlement between the left and the right side of the church in the area between the apse and the belltower. Such a settlement is confirmed by the significant inclination (downwards to the left) of the tie-rods of sections DD' and EE'. The absence of a significant vertical displacement at the springings of the arch in section EE' does not contrast with the occurrence of the abovementioned differential foundation settlement, as the original springings of this arch were restored over time and, thus, potential movements occurred in the past may have been hidden.

The deformation analysis of the right chapel of San Carlo Borromeo church is presented in Fig. 9. The analysis of section GG' (Fig. 9a) shows a rotation of both walls and floor in the direction of the landslide. The rotation of the floor ($\pi = 1.24°$) corresponds to a vertical displacement of 9 cm and is in full accordance with the settlement of the floor detected in section HH' (9 cm, see Fig. 9b). This outcome clearly indicates that the right chapel experienced a settlement of about 9 cm in correspondence of the southern corner.

To further investigate the differential settlements of the church, a displacement analysis of the floor of the nave was performed. An additional Grasshopper script was specifically designed for this purpose (see Fig. 10). With the aim of highlighting the out-of-plane deformations of the floor (which can be hidden by the significant rotations previously discussed), a tilted plane representing an

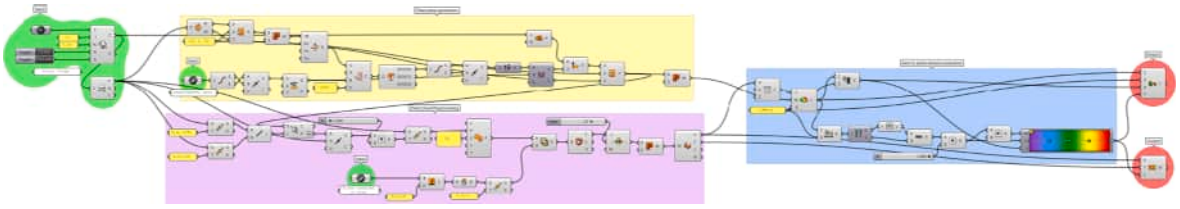

Fig. 10. Grasshopper script for the deformation analysis of the floor. Green: inputs; yellow: tilted plane generation; purple: point cloud pre-processing; blue: displacement evaluation; red: outputs used in Fig. 11. (For interpretation of the references to colour in this figure legend, the reader is referred to the web version of this article.)

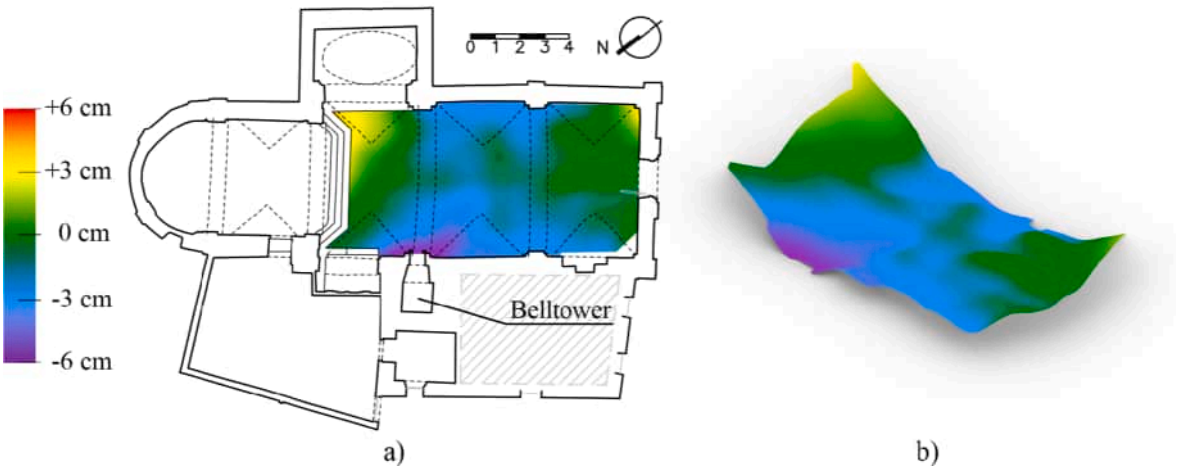

Fig. 11. Displacement analysis of the floor of the nave (represented in terms of out-of-plane displacements): a) plan; b) amplified 3D representation.

ideal configuration of the current geometry of the floor was used as reference plane. This tilted plane was obtained through a fitting operation on the surveyed point cloud of the floor, which was assumed, for this purpose, to be rotated only in the landslide direction, corresponding to the longitudinal axis of the church (yellow block in the script shown in Fig. 10). The inclination of the reference tilted plane obtained from the fitting operation was 1.15°, which is in close agreement with the rotation of the floor shown in Fig. 6 ($\delta = 1.16°$). Once the reference plane had been identified, some pre-processing of the point cloud was performed to reduce the number of points and arrange them in a regular grid (purple block in Fig. 10). The distance of each point from the reference plane was then computed and plotted (blue block in Fig. 10).

Fig. 11 shows the results of the above-described procedure. A localized settlement can be observed in correspondence of the belltower, in good agreement with the vertical displacement observed at the left springing of the transverse arch in section DD'. The smaller vertical displacement detected in the floor (6 cm) with respect to the arch (11 cm) can be explained by the fact that the floor was refurbished in the mid twelfth century.

In conclusion, the deformation analysis led to the identification of three main phenomena: (i) a global rotation of the entire church towards valley in the direction of the landslide; (ii) a vertical settlement of the left side of the church with respect to the right side (equal to about 5 cm in the apse and presbytery and 11 cm in correspondence of the belltower); (iii) a vertical settlement of about 9 cm in the right chapel at the southern corner.

3.3. Critical damage assessment and identification of displacement fields

With the aim of identifying the causes of damage, the crack patterns and deformations detected in San Carlo Borromeo church were critically analysed taking into consideration the damage mechanisms of historic masonry churches exposed to slow-moving landslides first identified in [8] and shown in Fig. 12. These damage mechanisms are global and involve the church in its entirety. Each mechanism is produced by a specific soil displacement pattern induced by the slow-moving landslide (either vertical or horizontal) and is associated to specific crack patterns and deformations.

Considering the damage mechanisms shown in Fig. 12, the global rotation of the buildings towards valley (Fig. 6) can be attributed to the vertical component of the slow-moving landslide movement. The cracks in the floor oriented perpendicular to the landslide direction (coloured in blue in Fig. 5c) and the vertical cracks in the longitudinal walls (Fig. 5b) can instead be attributed to the horizontal component of the landslide movement. These cracks clearly indicate that the church suffered an extension in the direction of the slow-moving landslide (see Fig. 12d). When an extension mechanism takes place, vertical cracks propagating from the level of the

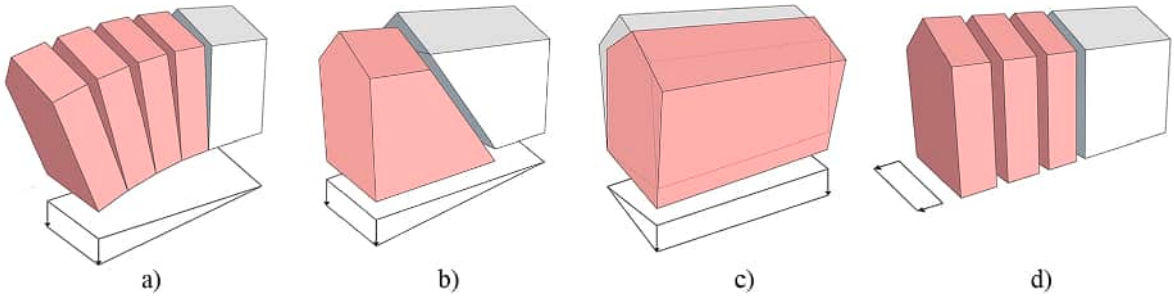

Fig. 12. Damage mechanisms of historic masonry churches exposed to slow-moving: a) hogging, b) shear deformation, c) global rigid rotation, d) extension [8].

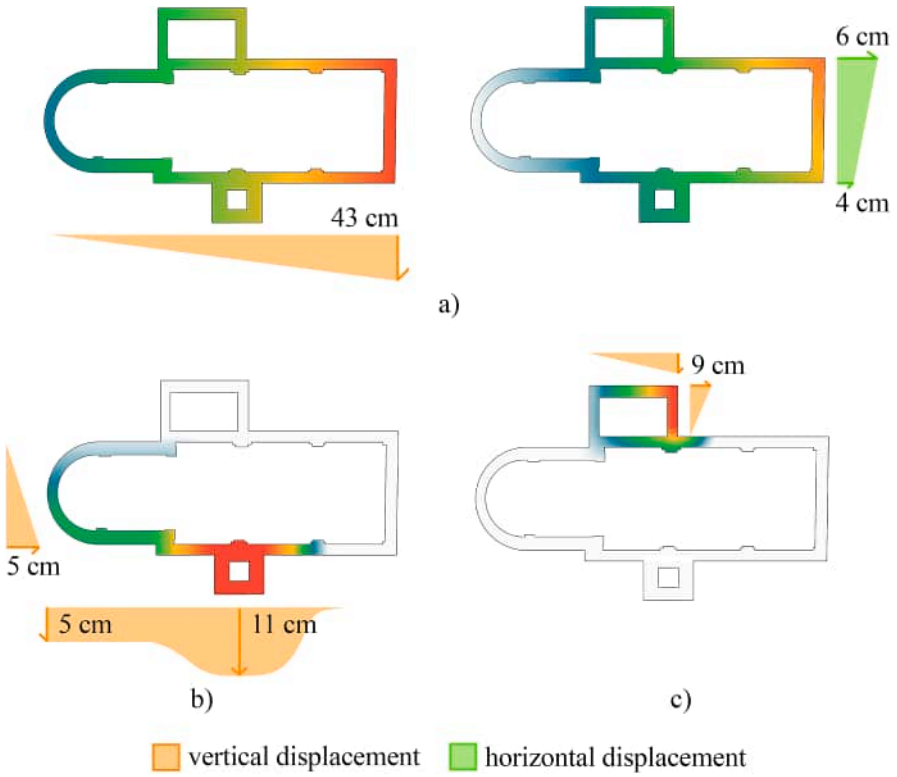

Fig. 13. Displacement fields: a) global displacement produced by the slow-moving landslide (on the left vertical component, $u_{global,v}$; on the right horizontal component, $u_{global,h}$); b) local vertical settlement of the left side of the church ($u_{left,v}$); c) local vertical settlement of the right chapel ($u_{right,v}$).

ground are expected to appear in both the longitudinal walls of the church in planes almost perpendicular to the landslide direction [8]. The presence of both vertical and diagonal cracks in the longitudinal walls of San Carlo Borromeo church (Fig. 5a-b) can thus be attributed to the combined action of the slow-moving landslide and foundation settlements. The effect of foundation settlements is particularly evident in the left longitudinal wall, which exhibits diagonal cracks propagating upwards at both sides of the belltower (Fig. 5a). These cracks indicate a settlement of the belltower, which is full agreement with the settlement detected through the deformation analysis (Section 3.2).

Looking at the types of damage shown in Fig. 12 and considering the direction of the slow-moving landslide affecting Cassingheno village, which is parallel to the direction of the longitudinal axis of San Carlo Borromeo church, the cracks in the vaults can hardly be attributed to the slow-moving landslide. Being oriented in the same direction as the landslide or exhibiting a concentric pattern around the belltower, they can indeed be attributed to differential foundation settlements and, in particular, to the larger settlement of the left side of the building with respect to the right side. Although no information about the soil under San Carlo Borromeo church is available, it is reasonable to assume that the differential foundation settlements may have been caused by heterogeneities of the soil and/or differences in the process of soil consolidation under the different parts of the building. It is likely that these foundation settlements are also responsible for the damage and deformations of the transverse arches (Fig. 7) and the differential vertical

displacements between the different parts of the building. Slow-moving landslides, indeed, do not produce such a localized damage [8].

Based on the previous considerations, the displacements produced at the base of the church by the slow-moving landslide and foundation settlements, which are responsible for damage and deformations, can be represented through three displacements fields, one global, affecting the entire church (Fig. 13a), and two local (Fig. 13b-c). The global displacement corresponds to the displacements induced by the slow-moving landslide and has both vertical ($u_{global,v}$) and horizontal ($u_{global,h}$) components (see Fig. 13 on the left and on the right, respectively). The local displacements represent the vertical settlements of the left side of the church ($u_{left,v}$, Fig. 13b) and the right chapel ($u_{right,v}$, Fig. 13c). The value of the vertical component of the global displacement ($u_{global,v}$) was estimated based on the rotation measured along the length of the nave ($\delta = 1.16°$), which was extended to the entire building (see angle Δ in Fig. 6). In such a way, a vertical displacement of 43 cm between the apse and the façade was obtained (Fig. 13a on the left). The value of the horizontal component ($u_{global,h}$) was taken equal to the sum of the width of the cracks in the floor of the nave, which was found to be slightly different on the left (4 cm) and right (6 cm) sides of the building (Fig. 13a on the right). The values of the vertical settlement of the left side of the building and the right chapel were taken equal to the values estimated through the deformation analysis (see Section 3.2).

4. Structural analysis

Structural analysis was performed with the dual objective of identifying the causes of the damage and deformations observed in San Carlo Borromeo church and evaluating if the displacements fields assessed through the deformation analysis were realistic and could be responsible for the current damage state. For these purposes, a FE model of the church in its undeformed configuration was prepared (Section 4.1), and nonlinear static analyses were performed by applying at the base of the structure the displacement fields identified in 3.3 (Section 4.2). The crack patterns and deformations predicted numerically were then compared with the real ones surveyed on site (Section 4.2).

4.1. Numerical model

4.1.1. Preparation of the FE model

Starting from the point cloud obtained from the laser scanner survey (Fig. 14a), a three-dimensional geometrical model of San Carlo Borromeo church (Fig. 14b) was created in Rhinoceros [27] and Ansys SpaceClaim [28]. The model did not include the clergy house, the sacristy, and the left chapel, as the first two (not accessed during the inspections) do not have structural continuity with the walls of the church and the third was created within the space of the sacristy by adding very thin brick walls without a load-bearing capacity. Due to the lack of information about the foundations of San Carlo Borromeo church, all the walls of the building were assumed to be founded at the same level (about one meter below the level of the floor of the nave). The undeformed reference configuration of the church was obtained by assuming that: (i) the walls were straight, vertical, and parallel in pairs; (ii) the tie-rods were horizontal; (iii) the arches had the elliptical undeformed geometry reconstructed in Section 3.2. The vaults were reconstructed starting from the undeformed geometry of the arches connected to them.

Starting from the geometrical model shown in Fig. 14b, a FE model of the church was created in Ansys Mechanical [29] (Fig. 14c). The timber structure of the roof was not included in the numerical model due to the lack of a proper survey. Based on the information on the roof structure provided in [30], the loads transferred by the roof to the underlying masonry structures were calculated and applied as distributed loads at the top the walls and point loads at the extrados of the vaults. No prestress was considered for the tie-roads due to the lack of detailed information on these metallic elements.

A macro-modelling approach was adopted to represent masonry, which was considered as a homogeneous material. The masonry walls and vaults as well as the metallic tie-roads were modelled through ten-nodes quadratic tetrahedrons solid elements (TET10,

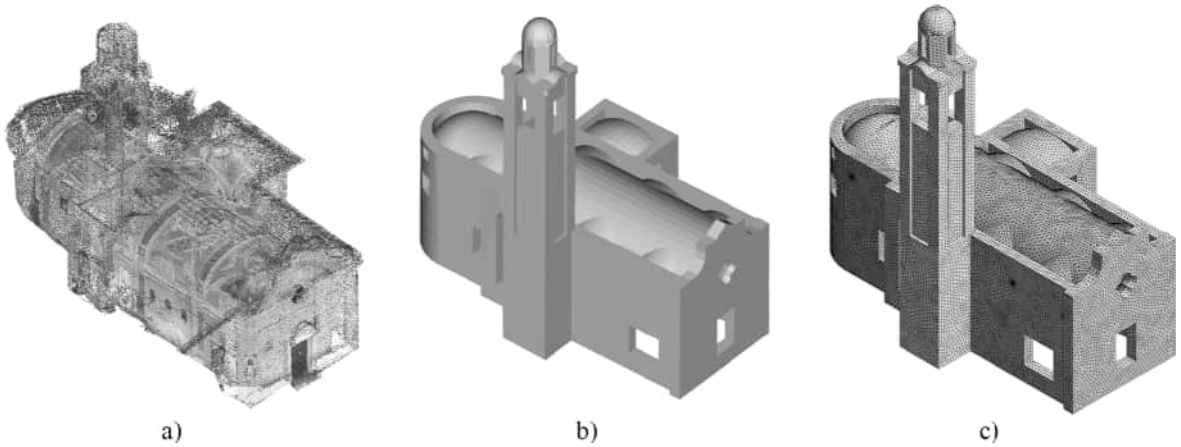

Fig. 14. A) point cloud, b) geometrical model, c) fe model.

Table 1
Material properties adopted for the stone masonry of walls and vaults.

E [GPa]	ν [-]	ρ [kg/m^3]	f_{uc} [Mpa]	f_{bc} [Mpa]	f_{ut} [Mpa]
1.5	0.18	2050	2.6	3.0	0.46

Table 2
Material properties adopted for the steel of the tie-rods (where σ_0 is the Yield stress and E_t is the tangent modulus).

E [Gpa]	ν [-]	ρ [kg/m^3]	σ_0 [Mpa]	E_t [Gpa]
210	0.3	7850	250	1.45

[29]). A mesh size of about 20 cm was adopted for the masonry elements. The mesh was refined at the contact surfaces between masonry and tie-roads to obtain an accurate stress representation. A mesh size of about 1 cm was used for the tie-rods. In total, the numerical model consisted of about 1.1 million nodes and 700 thousand elements (Fig. 14c). All the translational degrees of freedom of the nodes at the base of the church were restrained to provide boundary conditions.

4.1.2. Constitutive models and material properties

A perfectly elastoplastic model with a Drucker-Prager yield criterion was adopted for the masonry elements. Due to the lack of experimental data, the mechanical properties of the masonry were estimated based on the reference values suggested in the explanatory note of the Italian Building Code (Circolare no.7 of 2019, hereafter defined *Circolare* [31]) as well as on empirical relations from literature. More in detail, the Young's modulus E and the uniaxial compressive strength f_{uc} were taken equal to the minimum values provided by the Italian *Circolare* for ashlar stone masonry. The volumetric density ρ suggested for this type of masonry was adopted. The Poisson's ratio ν was taken equal to 0.18. To use the Drucker-Prager yield criterion implemented in Ansys Mechanical [29], values of biaxial compressive strength f_{bc} and uniaxial tensile strength f_{ut} had to be defined. These values were evaluated based on the following relations [32]:

$$f_{bc} = 1.5 f_{uc} \tag{1}$$

$$f_{ut} = 1.4 (f_{uc}/10)^{2/3} \tag{2}$$

The physical and mechanical properties adopted for the stone masonry of walls and vaults are reported in Table 1.

A bilinear isotropic hardening model was used to describe the mechanical behaviour of the steel of the tie-rods. Table 2 reports the material properties adopted for this steel.

4.2. Nonlinear static analyses

Nonlinear static analyses were performed to evaluate the structural performance of San Carlo Borromeo church under the action of the slow-moving landslide and differential foundation settlements. To this aim, the displacements fields identified in Section 3.2 were imposed at the base of the structure after the application of the self-weight. The vertical and/or horizontal displacements corresponding to each displacement field were applied at an incremental rate varying between 1/20 and 1/50 of the total displacement imposed in each step and were monotonically increased until reaching the value indicated in Fig. 13. The displacement fields were imposed according to the sequence shown in Fig. 15. The global vertical ($u_{global,v}$) and horizontal ($u_{global,h}$) displacements produced by the slow-moving landslide were applied in three steps (1, 2 and 3) after the application of the self-weight (step 0). In step 1, one third of $u_{global,v}$ *and* $u_{global,h}$ was imposed. Subsequently, in steps 2 and 3, one third of $u_{global,v}$ and $u_{global,h}$ was imposed in combination with the settlement of the left side of the building ($u_{left,v}$) and the settlement of the right chapel ($u_{right,v}$), respectively. The abovementioned sequence of application of the displacements fields was specifically chosen to take into consideration the history and construction phases of San Carlo Borromeo church. The global displacements were applied in all the steps after step 0 because it was assumed that the slow-moving landslide acted for the entire lifespan of the church, since its construction. This assumption is based on the fact the largest rotation in the direction of the landslide was detected in the apse, which is the most ancient part of the church (see Section 2.1). The settlement of the left side of the building was applied before that of the right chapel because the right chapel was built later than

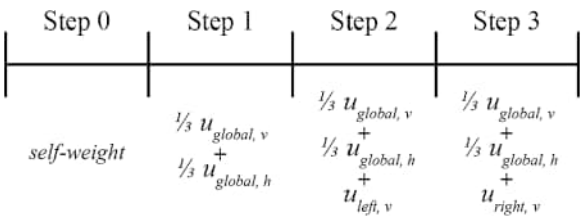

Fig. 15. Sequence of application of loads and displacement fields.

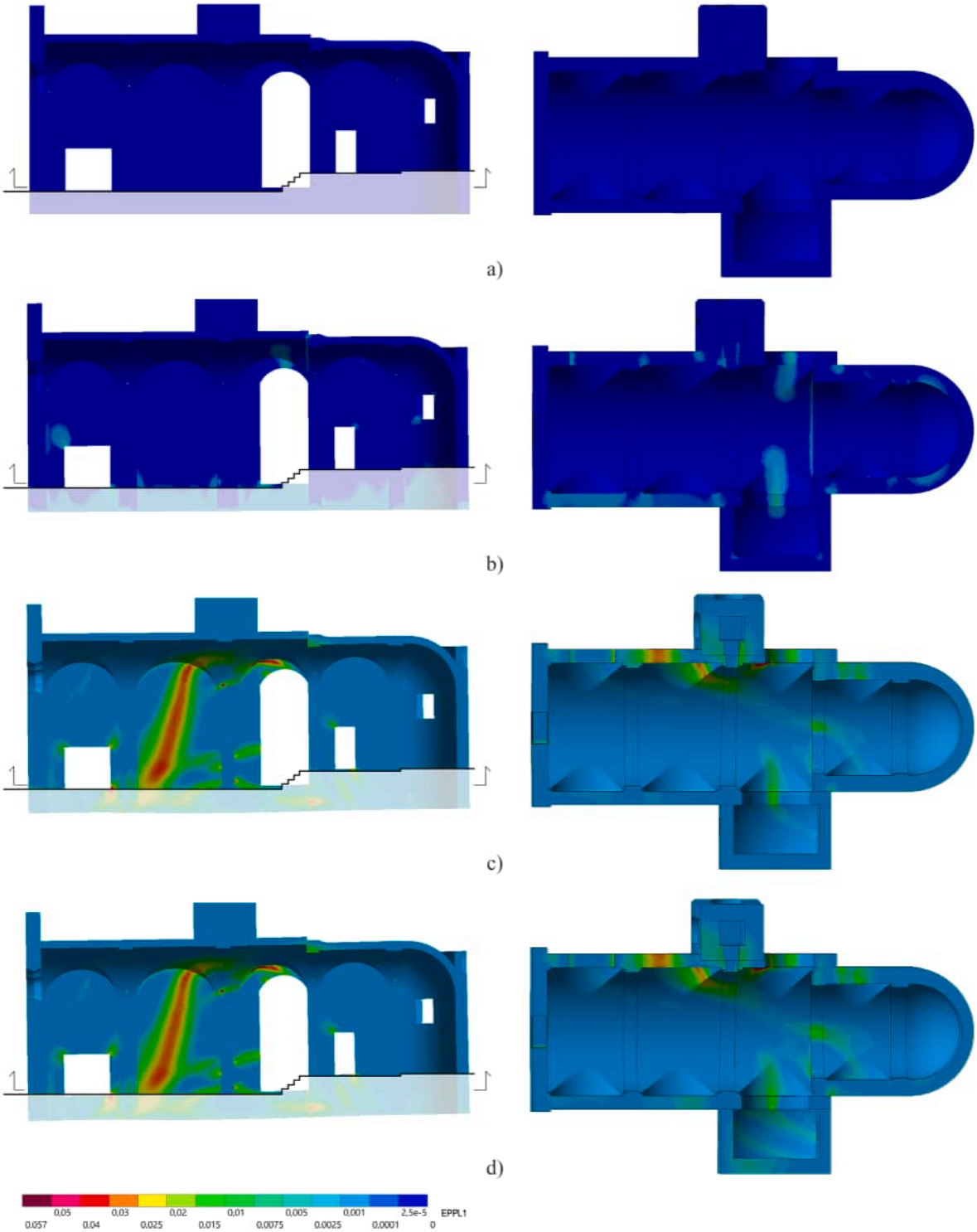

Fig. 16. Maximum principal plastic strain obtained at the end of each step of the sequence of loads and displacement fields identified in Fig. 15: a) step 0, b) step 1, c) step2, d) step 3. On the left: left side of the church (section AA'); on the right, plan (vaults and base of the walls, see the cutting plane line indicated on the left).

the other parts of the church (i.e., apse, presbytery, nave, and belltower). On the other hand, it should be noted that different sequences of application of the displacement fields were considered in [33]. However, no significant differences in terms of predicted damage and deformations were observed in these sequences after the application of all the considered displacement fields.

Fig. 16 shows the results obtained at the end of each step of application of the displacement fields in terms of maximum principal plastic strain, which provides an indication of the crack formation. The results are presented in elevation for the left side of the church (section AA'), which is the most representative (see Fig. 16 on the left), and in plan for the vaults and the base of the walls (see Fig. 16 on the right). The plan is obtained by cutting the numerical model approximately at the level of the floor of the nave (the cutting plane line is shown in Fig. 16 on the left). The application of the self-weight (step 0) did not produce any damage (Fig. 16a), while the application of the first third of the landslide-induced global displacements (step 1) resulted in limited damage (Fig. 16b), mostly localized at the base of the longitudinal walls and at mid-span of the arches that separate the nave from the lateral chapels (third bay behind the façade). As shown in Fig. 16c, the application of the settlement of the left side of the building and the second third of the global displacement (step 2) produced a significant worsening of the damage state of the church. Extensive cracks appeared in the left longitudinal wall as well as in the vaults of nave, presbytery, and right chapel. Conversely, the application of the settlement of the right chapel and the last third of the global displacements (step 3, Fig. 16c) did not significantly worsen the damage level, except in the right chapel, as expected, where further damage occurred in both walls and vaults. A vertical and diagonal crack also appeared in the right

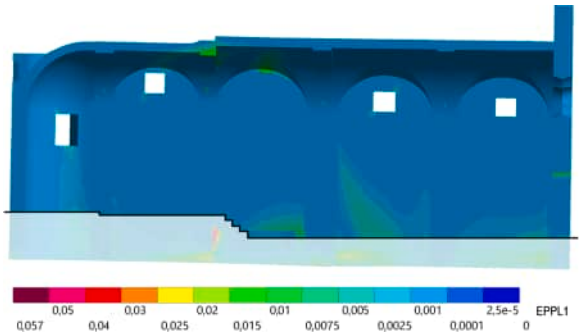

Fig. 17. Maximum principal plastic strain obtained in the right side of the church (section BB') at the end of the sequence of application of the loads and displacement fields identified in Fig. 15 (end of step 3).

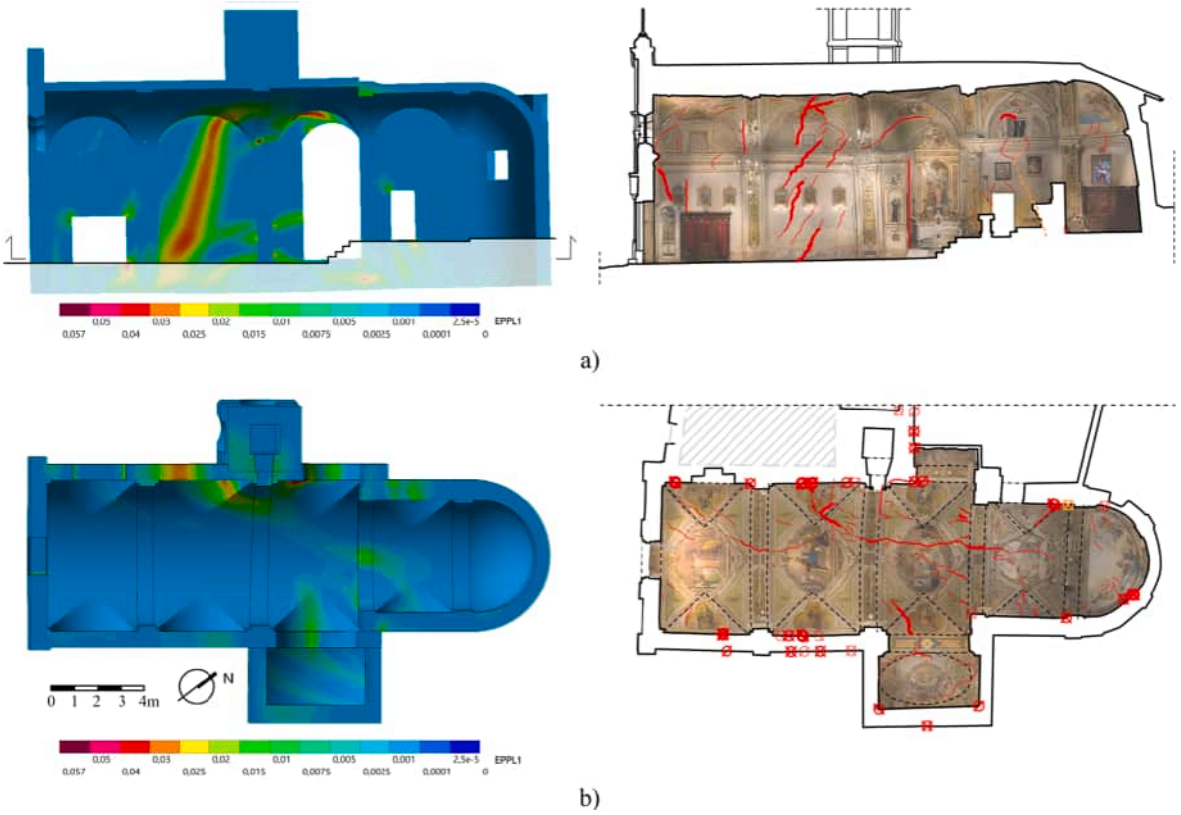

Fig. 18. Comparison between FE results (in terms of maximum principal plastic strain, on the left) and crack pattern surveyed on site (on the right): a) section AA' (left longitudinal wall), b) plan (vaults and walls).

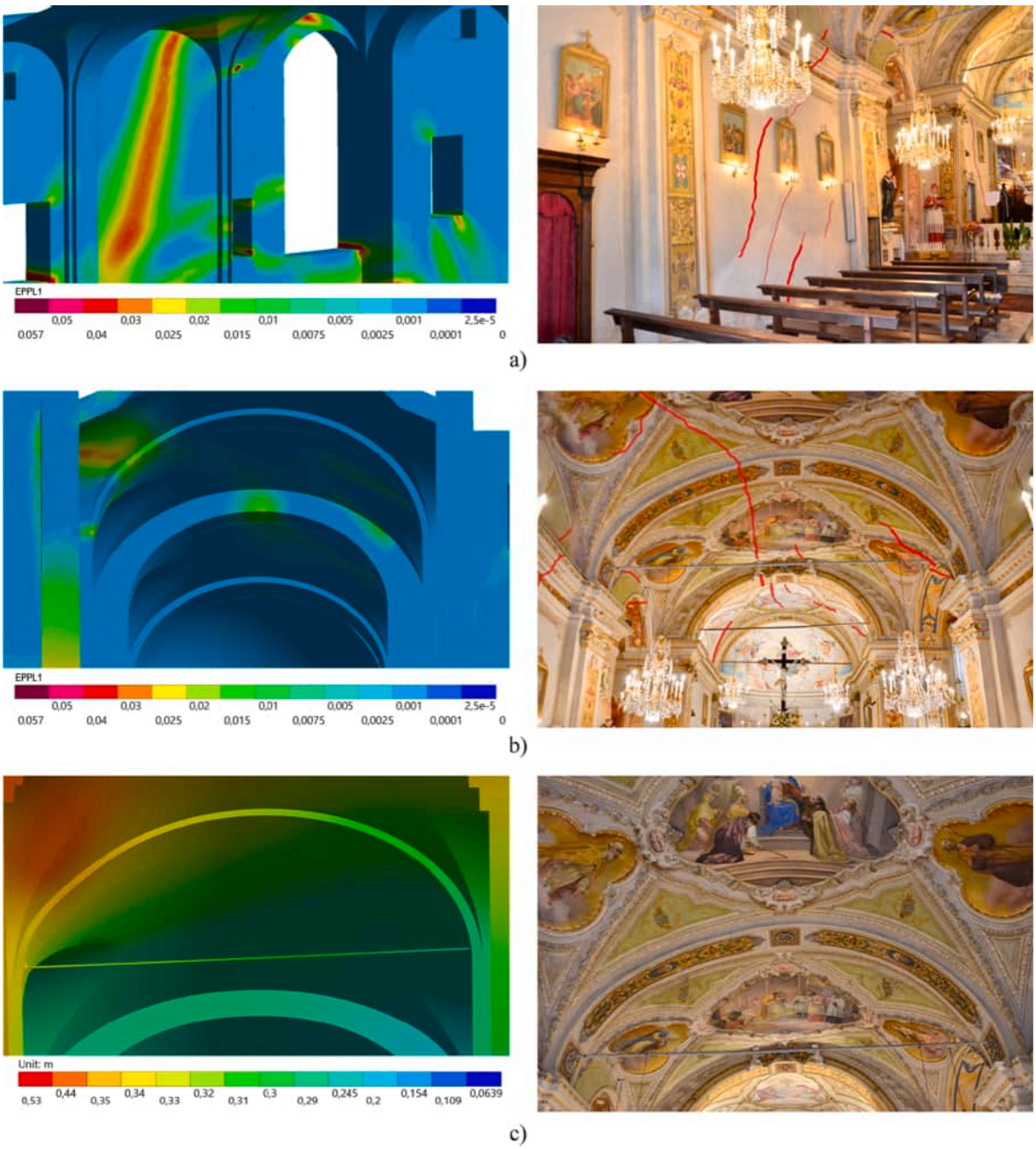

Fig. 19. Comparison between FE results [in terms of maximum principal plastic strain (a-b) or total displacement (c), on the left] and crack patterns and deformations surveyed on site (on the right): a) cracks in the left longitudinal wall, b) cracks in the vaults of the nave and presbytery, c) deformation of the second transverse arch behind the façade.

longitudinal wall, respectively in the apse and the second bay behind the façade (Fig. 17).

Fig. 18 and Fig. 19 provide a comparison between the damage predicted numerically and the crack patterns and deformations surveyed on site. The numerical model accurately reproduced the cracks in the walls, in particular the large diagonal cracks observed in the left longitudinal wall in the second bay behind the façade (Fig. 18a and Fig. 19a). The occurrence of the damage in the form of widespread plastic deformations instead of a series of well-defined cracks (as observed in the real building) is simply due to the constitutive model adopted for masonry. Since it is perfectly elastoplastic and does not include softening, it is not able to reproduce distinct cracks. As for the damage in the right longitudinal walls, the numerical model correctly predicted the occurrence of a vertical crack in the apse and diagonal cracks in the second bay of the nave behind the façade (compare Fig. 5b and Fig. 17). However, the low values of maximum principal plastic strain indicate that the severity of the real damage was underestimated. The cracking pattern

affecting the vaults of nave and presbytery and the cracks at mid-span of the arches separating nave and lateral chapels were also accurately simulated by the numerical model (see Fig. 18b and Fig. 19b). Lastly, the significant deformation and vertical settlement of the left springing of the second transverse arch behind the façade were accurately predicted (Fig. 19c).

The good agreement between the predicted and real damage and deformations proved the capacity of the numerical model to simulate the current damage state of San Carlo Borromeo church as well as the accuracy of the displacement fields estimated through the deformation analysis. The damage patterns obtained at each step of application of the displacement fields also allowed some conclusions about the causes of damage to be put forward. First, the settlement of the left part of the church was found to be responsible for the diagonal cracks of the longitudinal walls, the cracks in the vaults and the settlement of the left springings of the transverse arches, which is in full accordance with the hypotheses on the causes of damage made in Section 3.3. Second, such a settlement produced most of the damage observed in the building, while the slow-moving landslide resulted in localized slight damage. In this respect, it should be noted that the damage in the floor attributed to the slow-moving landslide (extension mechanism) could not be reproduced to the lack of a floor in the FE model.

5. Conclusions

The structural damage assessment of cultural heritage buildings requires to take into account the building history, actual geometry, past and present actions, and current damage and deformations. In this paper, the structural damage assessment of San Carlo Borromeo church, a historic masonry building affected by slow-moving landslides, was performed by combining structural analysis with historical research, on-site inspections, laser scanner survey and deformation analysis.

The historical research allowed the history, construction phases and architectural/structural alterations of the church to be identified. The on-site inspections supplied information about geometric features, structural details and materials and allowed the crack patterns to be surveyed and mapped in detail. The laser scanner survey provided the actual geometry of the church with a high level of accuracy. The deformation analysis led to the identification of the deformations and displacements experienced by the church during its lifespan.

A critical analysis of crack patterns and deformations allowed the potential causes of damage to be identified. Differential foundation settlements were found to have occurred in combination with the slow-moving landslide affecting the building. Thanks to the deformation analysis, displacement fields representative of the displacements produced by the two-above mentioned phenomena were identified. Such displacement fields were used to perform structural analysis and numerically assess the structural response of the building through nonlinear static analyses. For this purpose, a FE model of the church in its deformed geometric configuration was prepared.

Although the constitutive model adopted for masonry did not allow distinct cracks to be reproduced, the comparison between the damage predicted numerically and that observed on site showed good agreement. This confirmed the hypotheses on the causes of damage made through the critical damage assessment and demonstrated the capability of the numerical model to capture the current damage state. The accuracy of the displacement fields assessed by the deformation analysis and adopted in the nonlinear-static analyses was also proved. In view of this, the deformation analysis can be considered an effective tool to support structural analysis and assess the deformations and displacements experienced by historic masonry structures over time.

In future works, further numerical simulations will be performed by adopting a masonry constitutive model that includes softening and allows single cracks to be more accurately reproduced.

Declaration of Competing Interest

The authors declare that they have no known competing financial interests or personal relationships that could have appeared to influence the work reported in this paper.

Data availability

The data that has been used is confidential.

Acknowledgements

The authors would like to acknowledge Prof. Rita Vecchiattini from the University of Genoa (Italy) for the support provided during on-site inspections.

Statements and Declarations

The authors declare that they have no known competing financial interests or personal relationships that could have appeared to influence the work reported in this paper.

References

[1] Roca, P., 2004. Considerations on the significance of history for the structural analysis of ancient constructions. *Proceedings of IV Structural analysis of historical constructions*, ed. Lourenço, P., Modena, C., Roca, P., pp. 63-73, Balkema, Amsterdam.

[2] P. Roca, M. Cervera, G. Gariup, L. Pelà, Structural analysis of masonry historical constructions. Classical and advanced approaches, Archives of Computational Methods in Engineering 17 (3) (2010) 299–325, https://doi.org/10.1007/s11831-010-9046-1.

[3] Roca, P., Lourenço, P.B. and A. Gaetani. 2019. *Historic Construction and Conservation. Materials, Systems and Damage*. Routledge: New York.

[4] P. Roca, M. Cervera, L. Pelà, M. Chiumenti, Continuum FE models for the analysis of Mallorca Cathedral, Engineering Structures 46 (2013) 653–670, https://doi.org/10.1016/j.engstruct.2012.08.005.

[5] Y. Yardım, E. Mustafaraj, Effects of soil settlement and deformed geometry on a historical structure, Natural Hazards and Earth Systems Sciences 15 (2015) 1051–1059, https://doi.org/10.5194/nhess-15-1051-2015.

[6] Saloustros, S., Pelà, L., Roca, P., and J. Portal. 2014. Assessment of structural damage in historical constructions using numerical models: the case of the church of the Poblet Monastery. *SAHC 2014: Proceedings of the 9th International Conference on Structural Analysis of Historical Constructions*.

[7] S. Saloustros, L. Pelà, P. Roca, J. Portal, Numerical analysis of structural damage in the church of the Poblet Monastery, Engineering Failure Analysis 48 (2015) 41–61, https://doi.org/10.1016/j.engfailanal.2014.10.015.

[8] C. Ferrero, L. Cambiaggi, R. Vecchiattini, C. Calderini, Damage Assessment of Historic Masonry Churches Exposed to Slow-moving Landslides, International Journal of Architectural Heritage 15 (8) (2021) 1170–1195, https://doi.org/10.1080/15583058.2020.1799259.

[9] Ferrero, C., Cambiaggi, L., Calderini, C. and R. Vecchiattini. 2022. Historic masonry churches exposed to slow-moving landslides: a critical damage assessment. *Geotechnical engineering for the preservation of monuments and historic sites III*, ed. R. Lancellotta, C. Viggiani, F. De Silva, and L. Mele. London: CRC Press/ Balkema.

[10] P. Lacroix, A.L. Handwerger, G. Bièvre, Life and death of slow-moving landslides, Nature Reviews Earth & Environment 1 (2020) 404–419, https://doi.org/10.1038/s43017-020-0072-8.

[11] Cruden, D. M., and D. J. Varnes. 1996. Landslide types and processes. *Landslides: investigation and mitigation, Transportation Research Board,* Special Report 247, 36–75. National Academy of Sciences, Washington, D.C.

[12] S. Ferlisi, G. Gullà, G. Nicodemo, D. Peduto, A multi-scale methodological approach for slow-moving landslide risk mitigation in urban areas, southern Italy. *Euro-Mediterranean Journal for Environmental*, Integration 4 (20) (2019), https://doi.org/10.1007/s41207-019-0110-4.

[13] Nicodemo, G. 2017. Vulnerability analysis of buildings in areas affected by slow-moving landslides and subsidence phenomena. PhD dissertation, University of Salerno.

[14] Nicodemo, G., S. Ferlisi, D. Peduto, L. Aceto, and G. Gullà. 2020. Damage to masonry buildings interacting with slow-moving landslides: A numerical analysis. *Geotechnical research for land protection and development. CNRIG 2019. Lecture notes in Civil Engineering*, ed. F. Calvetti, F. Cotecchia, A. Galli, and C. Jommi, vol. 40, 52–61. Cham: Springer. 10.1007/978-3-030-21359-6_6.

[15] D. Peduto, G. Nicodemo, M. Caraffa, G. Gullà, Quantitative analysis of consequences to masonry buildings interacting with slow-moving landslide mechanisms: A case study, Landslides 15 (2018) 2017–2030, https://doi.org/10.1007/s10346-018-1014-0.

[16] D. Reale, C. Noviello, S. Verde, L. Cascini, G. Terracciano, L. Arena, A multi-disciplinary approach for the damage analysis of cultural heritage: The case study of the St. Gerlando Cathedral in Agrigento, Remote Sensing of Environment 235 (2019), 111464, https://doi.org/10.1016/j.rse.2019.111464.

[17] Ferrero, C., Cambiaggi, L., Fenialdi, A., Roca, P., Vecchiattini, R. and C. Calderini. 2021. Slow-moving landslide damage assessment of historic masonry churches: some case-studies in Italy. *SAHC 2021: Proceedings of the 12th International Conference on Structural Analysis of Historical Constructions*, ed. P. Roca, L. Pelà and C. Molins. Cornellà de Llobregat: Artes Gráficas Torres S.L.

[18] Cambiaggi, L., Ferrero, C., Riccardo, B., Vecchiattini, R., and C. Calderini. 2021. Effect of Slow-Moving Landslides on Churches in the Liguria Region: a Geotechnical Approach. In P. Roca, L. Pelà and C. Molins (eds.) *SAHC 2021: 12th International Conference on Structural Analysis of Historical Constructions*; Online event, 29 September-1 October 2021. Cornellà de Llobregat: Artes Gráficas Torres S.L.

[19] Ferrero, C., Berardi, R., Calderini, C., Cambiaggi, L., and Vecchiattini, R. 2022. A geotechnical analysis to assess the effect of slow-moving landslides on historic masonry churches. *International Journal of Architectural Heritage* (Special Issue of selected papers from the 12th International Conference on Structural Analysis of Historical Constructions, SAHC 2021). 10.1080/15583058.2022.2125354.

[20] Cazzulo, P., Barbieri, R. and F. Tirini. 1998. *Carpeneto - Una piccola, grande Comunità.*

[21] A.C. Sanguigliani, L'agro Vogherese. Memorie sparse di storia patria, Casorate Primo: Rossi. 3 pag. 348 (1891).

[22] Archivio Diocesano, 2020. Written documents from the Diocesan Archive (Archivio Diocesano) of the city of Tortona. Last accessed in 2020 (In Italian).

[23] Dipartimento della Protezione Civile, 2022. Seismic classification updated to December 31st, 2022. https://rischi.protezionecivile.gov.it/static/2074f6ab2b2a459da2507e43dcb30e37/mappa-classificazione-sismica-aggiornata-al-31-dicembre-2022.pdf. Last accessed on January 7th, 2023.

[24] Arpal 2020. *Banca dati ReMoVer - Commento generale all'attività di monitoraggio.* Accessed September 20, 2021. https://srvcarto.regione.liguria.it/dtuff/img/Remover/Commenti_Siti/GE026_commento_tot.pdf.

[25] Federici, P. R., M. Capitani, A. Chelli, N. Del Seppia, and A. Serani. 2004. *Atlante dei Centri Abitati Instabili della Liguria. II. Provincia di Genova* (*Atlas of the Unstable Inhabited Centers of Liguria*. II. Genova province). Regione Liguria, Genova, Italy.

[26] Autorità di bacino distrettuale del fiume Po, 2017. *Atlante dei Rischi Idraulici e Idrogeologici* (Atlas of Hydraulic and Hydrogeological Risks). Accessed October 25, 2018. http://www.pai.adbpo.it/.

[27] Robert McNeel & Associates. 2018. "Rhino 6 User manual".

[28] Ansys inc. 2020b. Discovery SpaceClaim, Release 2020 R2.

[29] Ansys inc. 2020a. Mechanical User's Guide, Release 2020 R2.

[30] Varese, G.B. 2015. *Progetto di rifacimento del manto di copertura.*

[31] Ministero delle infrastrutture e dei trasporti. Circolare 21 gennaio 2019, n.7. *Istruzioni per l'applicazione dell'«Aggiornamento delle "Norme tecniche per le costruzioni"» di cui al decreto ministeriale 17 gennaio 2018*.

[32] H. Jiang, J. Zhao, Calibration of the continuous surface cap model for concrete, Finite Elements in Analysis and Design. 97 (2015) 1–19, https://doi.org/10.1016/j.finel.2014.12.002.

[33] Cabella, C., and G.L.S Sacco. 2021. Studio degli effetti di una frana attiva su un edificio voltato: la chiesa di San Carlo Borromeo in Cassingheno (Genova). Master thesis, University of Genoa (in Italian).